

Identifying Proteins of High Designability via Surface-Exposure Patterns

Eldon G. Emberly¹, Jonathan Miller¹, Chen Zeng², Ned S. Wingreen¹, and Chao Tang^{1,*}

¹*NEC Research Institute, 4 Independence Way, Princeton, NJ 08540, USA*

²*Department of Physics, George Washington University, Washington, D. C. 20052, USA*

* *Corresponding author: email: tang@research.nj.nec.com P: (609) 951-2644 F: (609) 951-2496*

Keywords: protein design, protein structure prediction, off-lattice model, hydrophobicity

ABSTRACT

Using an off-lattice model, we fully enumerate folded conformations of polypeptide chains of up to $N = 19$ monomers. Structures are found to differ markedly in *designability*, defined as the number of sequences with that structure as a unique lowest-energy conformation. We find that designability is closely correlated with the pattern of surface exposure of the folded structure. For longer chains, complete enumeration of structures is impractical. Instead, structures can be randomly sampled, and relative designability estimated either from designability within the random sample, or directly from surface-exposure pattern. We compare the surface-exposure patterns of those structures identified as highly designable to the patterns of naturally occurring proteins.

I. INTRODUCTION

Naturally occurring proteins fold into specific three-dimensional structures to achieve their unique functionality.¹ For many proteins, it has been shown that the amino-acid sequence alone is sufficient to determine the folded conformation.² Interestingly, out of all geometrically possible folds, nature seems to have selected only a small set of fold families.^{3–6} This selection may arise, in part, from differences in the *designability* of folded structures.^{7–10} By definition, the designability of a structure is the number of amino-acid sequences with that structure as the lowest-free-energy conformation. In lattice models, where it is possible to enumerate all compact structures, there exists a small class of highly designable structures, *i.e.* structures which are unique lowest-energy conformations of many more than their share of sequences.^{10,11} The sequences associated with these highly designable structures are found to have protein-like properties: mutational stability,^{9,10} thermodynamic stability,^{10,11} and fast folding kinetics.¹² The topology of the neutral networks formed by the sequences of designable lattice model structures have also received study.¹³ Recently, off-lattice studies of protein structures have also shown that certain backbone configurations are highly designable, and that the associated sequences have enhanced mutational and thermodynamic stability.¹⁴ Therefore, whether one’s goal is to better understand existing protein fold families or to design novel folds,¹⁴ designability may offer a way to identify structures and sequences with protein-like folding properties.

In previous work, the determination of a structure’s designability has relied upon the enumeration of a wide cross section of all possible structures. This is because the designability of one structure depends on competition for sequences from other structures. For short chains on lattices it is straightforward to enumerate all compact structures.^{15–19,9,10} For off-lattice models, one approach has been to enumerate all structures obtainable with a small, discrete set of backbone dihedral angles.¹⁴ Clearly, for long peptide chains, this complete enumeration is infeasible, even for a small set of dihedral angles. Can one nevertheless identify highly designable long-chain protein structures?

In this paper, we present evidence from studies of short chains, up to $N = 19$, that the designability of a structure can be predicted without a complete enumeration of structures. Essentially, this is possible because we have found that the designability of a structure is closely connected to its pattern of surface exposure. Structures with large variation in surface exposure are likely to be highly designable, structures with more uniform surface exposure are not. The higher the designability of a structure, the more clearly differentiated are its surface and core. Because the variation in surface exposure of a structure is independent of all other structures, designability can be estimated structure by structure without the need for complete enumeration.

One implication of this result is that candidates for highly designable *long-chain* structures can be identified simply from their surface-exposure patterns. This approach avoids the need for a complete enumeration of structures. It is therefore computationally feasible to consider much longer peptide chains, with a greater variety of backbone conformations. We demonstrate the efficiency of this approach by generating backbone configurations of up to $N = 40$ monomers. For these lengths, complete enumeration of structures would be impractical. Instead, we generate a relatively sparse sample of structures. From among the sample it is straightforward to select the candidate highly designable conformations as those

with the most clearly delineated surfaces and cores. An effectively equivalent procedure is to calculate designability allowing only the structures in the sparse sample to compete for sequences. In either case, successful prediction of designability relies on its close relation to surface-exposure variation – a property of individual structures. There is one important caveat to this point – two structures with very similar patterns of surface exposure will compete for structures often in a “winner-take-all” fashion. The implications of this for design are discussed in Sec. III on random sampling.

The results of the off-lattice model motivate us to consider the surface-exposure pattern of natural protein structures. We report a study of the surface-exposure pattern of backbones of up to length $N = 75$ from the Protein Data Bank. For small proteins, which are often stabilized by disulfide bonds and salt bridges, there is often no clearly delineated core. In contrast, for large proteins the core is uniformly well defined with little variation from structure to structure. The most highly designable configurations generated using our sampling technique have patterns of surface exposure that fall within the range of naturally occurring proteins.

II. MODELS AND METHODS

The designability of a structure is a measure of how many sequences “fold” into that structure in relation to all other competing structures. To precisely determine designability requires generating a comprehensive set of structures, which then compete as possible lowest-energy states for amino-acid sequences. It is only truly feasible to generate a complete set of model structures for short polypeptide chains. For larger chains, say with $N > 30$ monomers, it is not currently possible to enumerate structures. However, it will be shown below that it is possible to *estimate* the designability of structures without complete enumeration. To find the best means of estimating designability, we study short chains ($N = 15, 17,$ and 19) for which designability can be precisely determined within an off-lattice model. This section reviews our model for obtaining the designabilities of short-chain polypeptide structures. In the next section, we show that the designability of a structure within this model can be estimated from its surface-exposure pattern.

Off-lattice model – Our method of generating structures is closely related to the discrete-angle models introduced by Park and Levitt.^{20,14} For short polypeptide chains of $N = 15, 17,$ and 19 monomers, a “complete” set of backbones is generated using a fixed set of three dihedral (ϕ, ψ) angles.²⁰ For this particular study, we employ one angle-pair ($-60, -50$) from the alpha-helical region of a Ramachandran plot, and two angle-pairs ($-140, 150$) and ($-65, 125$) from the beta-strand region. The complete set of 3^N backbones is generated with these angles.

To restrict our consideration to self-avoiding structures, we introduce “side groups” by hard spheres of radius $r_\beta = 1.9\text{\AA}$ centered on the C_β positions. Self-avoidance is taken into account by discarding all structures with overlapping spheres. The percentage of self-avoiding structures out of the possible 3^N structures was found to be 42% for $N = 15$, 36% for $N = 17$ and 31% for $N = 19$.

An example of a structure generated using the three angle-pairs and with self-avoiding spheres centered on the C_β positions is shown in Fig. 1.

Hydrophobicity model – There is considerable evidence that hydrophobic forces are primarily responsible for the folding of an amino-acid sequence into a particular structure.^{21–23} The hydrophobicity of each type of amino acid can be determined experimentally.^{24–26} Those which are more hydrophobic are energetically favored to reside in the core of the folded protein, where there is low exposure to water. In a given folded protein, a hydrophobic energy can be assigned to each particular amino acid according to its hydrophobicity and its exposure to water.

To determine the hydrophobic energy of an amino-acid sequence folded into one of our model structures it is necessary to determine the exposure of each residue along the backbone. As described above, hard spheres are placed on each C_β position, and the surface exposure of these spheres to water is evaluated. This is done using the method of Shrake and Rupley²⁷ which determines how much of a sphere centered on a C_β position is exposed to a water molecule, which is represented as a sphere with a radius of 1.4 Angstroms. We use the notation that the j^{th} residue of the α^{th} structure has accessible surface area a_j^α . The sum of these surface areas gives the total residue accessible surface area for a given structure. As a screen, we use this quantity to remove those structures which have too much surface exposure and thus are too open to be stable folds. In practice, we reduce the representative set to approximately 5000 structures with the least exposed surface area.²⁸

These remaining structures are “compact” in that even for the small peptide chains used in this study ($N = 15, 17,$ and 19) there is the beginning of the formation of a core which is inaccessible to solvent. We then normalize the surface area of the remaining compact structures using the following normalization condition,

$$\tilde{a}_j^\alpha = \frac{a_j^\alpha}{\sum_j a_j^\alpha}. \quad (1)$$

The motivation behind this normalization procedure is that we wish the remaining compact structures to all be *equally* compact – the normalized structures all have the same total surface exposure ($\sum_j \tilde{a}_j^\alpha = 1$). This is in line with lattice studies where all structures are equally compact.^{9–11} The normalization eliminates the need for an overall compactification energy in the energy function used below since all structures are equally compact. Physically, the use of equally compact structures accounts for the tendency of each structure to relax to its best packed equivalent.

With the residue-by-residue surface areas of a set of compact, self-avoiding structures in hand, all that is needed is a hydrophobic-energy function to associate these structures with amino-acid sequences. We find it convenient to assign a *polarity* between 0.0 and 1.0 to each amino acid, with 0.0 being highly hydrophobic and 1.0 being highly polar. Our notation is that the j^{th} amino acid of a sequence β has polarity p_j^β . In our model, the energy of this amino-acid sequence when folded into the α^{th} structure is^{11,29,30}

$$E^{\beta,\alpha} = - \sum_j p_j^\beta \tilde{a}_j^\alpha. \quad (2)$$

For a given sequence, the lowest-energy structure is the one that minimizes this energy. Note that since all structures have the same total exposed surface ($\sum_j \tilde{a}_j^\alpha = 1$), a sequence will have lowest energy on the structure that best matches its *pattern* of hydrophobicity –

more hydrophobic at core sites, more polar at surface sites – independent of the absolute hydrophobicity or polarity of the sequence.

Designability – The designability of a given structure is defined as the number of sequences with that structure as a unique lowest-energy conformation.¹⁰ We assess the designabilities of structures by evaluating the energy (2) of a large number of random sequences of polarities on all the structures in the representative set. Each sequence of polarities p_j is generated as a string of N random real numbers between 0.0 and 1.0. Consistent with a previous study,¹⁴ we report in the next section that most structures are the lowest-energy conformations of only a few or no sequences, and hence these structures have low designability. Only a small fraction of structures are highly designable.

III. RESULTS AND DISCUSSION

We now examine the factors which influence a structure’s designability. What causes a structure to be the lowest-energy state of many sequences within our hydrophobic model? We show below that the *variance* of a structure’s surface-area pattern is an important quantity in determining designability.

Predictors of designability – In our model, the energy of a sequence folded into a particular structure is given by Eq. (2). Therefore, the only property of a structure which influences energy is the structure’s vector of solvent-exposed surface areas $\vec{a} = \tilde{a}_1, \dots, \tilde{a}_N$. Moreover, because of the normalization condition, Eq. (1), all such vectors reside on an N -dimensional hyper-plane (*e.g.* for a chain of length $N = 3$, the vectors would reside on the plane $\tilde{a}_1 + \tilde{a}_2 + \tilde{a}_3 = 1$). The vectors for all structures can be decomposed into a constant component $\vec{n} = (1/N, 1/N, \dots, 1/N)$ normal to this hyper-plane plus a variable in-plane component (see Fig. 2). We denote a structure’s in-plane component by $\vec{r} = \vec{a} - \vec{n}$. For a given sequence, the relative energies of structures depend only on these \vec{r} ’s, as can be seen by rewriting the hydrophobic energy as

$$E^{\beta,\alpha} = - \sum_j p_j^\beta r_j^\alpha - \frac{1}{N} \sum_j p_j^\beta, \quad (3)$$

where the last term is structure independent.

The first term in the energy (3) is the negative of an N -dimensional dot product between the polarity vector \vec{p} of the sequence and the in-plane component \vec{r} of the structure. The lowest-energy structure is the one for which this dot product is the greatest. The vector \vec{p} can also be written in terms of a component parallel to the normal vector \vec{n} of the hyper-plane and a component that lies in the hyper-plane. For a given sequence, the lowest-energy structure will be the structure that has the greatest projection of its in-plane component \vec{r} onto the in-plane component of the vector \vec{p} . Hence, structures that lie the farthest out from the “origin of the hyperplane”, \vec{n} , on this plane will tend to be lowest-energy structures for the most sequences (*e.g.*, structure “S” shown in Fig. 2). Distance from the origin \vec{n} on the hyper-plane is therefore expected to be an easy-to-calculate predictor of designability. For

a given structure this distance is

$$r = \sqrt{\sum_j (r_j)^2}. \quad (4)$$

Note that r^2/N is the variance of a structure’s residue-by-residue exposed surface area. From a physical point of view, the in-plane distance r is a measure of how much variation there is in a structure’s exposed surface area compared to uniform exposure to solvent. Structures that have large values of r have well differentiated core and surface sites.

However, designability is determined by more than just r . By definition, to be highly designable, a structure must be the lowest-energy state for a large number of sequences \vec{p} . For each of the structures with large r there exists a kind of “hyper-cone” of sequences \vec{p} for which it is the lowest-energy state^{11,30} (this is shown schematically by the shaded area in Fig. 2). The volume of this cone, and hence the designability of the structure, depends on the density of competing structures around it. This suggests that structures that lie farthest from other structures on the hyper-plane will be most designable. For example, a structure that is not the farthest out in its own direction will tend to be less designable because a farther out structure will be lower in energy for all sequences lying in the same direction. Hence, an improved predictor for designability is the distance of a structure from the center of the distribution of structures.³⁰ We denote this distance from the mean by

$$\sigma = \sqrt{\sum_j \sigma_j^2}, \quad (5)$$

where

$$\vec{\sigma} = \vec{r} - \langle \vec{r} \rangle, \quad (6)$$

and where $\langle \vec{r} \rangle$ is the mean of the distribution of exposure vectors in the plane,

$$\langle \vec{r} \rangle = \frac{1}{S_{\text{tot}}} \sum_{\alpha=1}^{S_{\text{tot}}} \vec{r}^\alpha, \quad (7)$$

with S_{tot} the total number of structures in the set. One can determine if a structure is the farthest out in its own direction by simply projecting all of the other $\vec{\sigma}$ ’s onto its own $\vec{\sigma}$. Structures that have a large distance from the mean and also lie the farthest out in their own direction are shown below to be highly designable. It has been previously shown in lattice models that the designability of a structure is inversely correlated with the density of other structures in its local neighborhood.¹⁰ However, to generate enough structures to adequately sample local densities essentially requires complete enumeration of structures. In contrast, the quantities \vec{r} and $\vec{\sigma}$ depend only upon a structure’s global position within the space and require sampling of relatively few structures to compute. Fig. 2 illustrates the quantities of interest, \vec{r} and $\vec{\sigma}$, for a particular structure that lies far from the origin on the hyper-plane. We now examine how these quantities correlate with designability for some specific cases.

Enumeration studies of 15, 17, and 19mers – The complete set of all self-avoiding compact structures was generated using the three angle set described in Sec. II for lengths $N = 15, 17$, and 19 . For each set of structures at a given length N , we evaluated designability using the enumeration method described in Sec. II, and ranked the structures from highest to lowest designability. In Fig. 3, the histogram of designability for the 17mer is shown. Consistent with other studies of designability, the histogram has an exponentially decreasing tail of highly designable structures.^{10,14} Most of the structures in the representative set have low designability, whereas only a few are highly designable.

The distances r and σ were also computed for all structures. The difference between the in-plane distance r and the distance from the mean σ arises from the fact that the mean exposure vector in the plane $\langle \vec{r} \rangle$ is not zero. In Fig. 4, the mean vector $\langle \vec{r} \rangle$ for the $N = 17$ case is shown. From the plot it is clear that the ends of a 17mer are on average more exposed to solvent than the central portion. For the other lengths studied the same behavior was found, namely, averaged over the representative set, the ends of the structures tend to be more exposed than the central portion.

Before looking at how designability correlates with σ and r , we briefly show how they relate to a structure’s compactness. In Fig. 5, a histogram of the in-plane distances r is shown for *all* self-avoiding 17mers (solid line) and the 5000 most compact 17mers (dashed line). The figure shows that our screen of structures for compactness removes most structures which have low values of r , but does not remove those that have high values of r . Hence structures that have a large in-plane distance r , *i.e.* large surface-exposure variation, are also compact.

Fig. 6 shows the correlation between the in-plane distance r and the distance from the mean σ , and how these relate to designability for the $N = 17$ case. There is a clear correlation between the two distances σ and r , but σ is a better predictor of designability. The top 50 designable structures are shown as black circles in Fig. 6. Most of the top 50 designable structures have values of $\sigma > 0.075$, and only a few less designable structures have σ values this high. In contrast, only about 10 out of the 50 topmost designable structures have values of $r > 0.075$, and for values less than this there is a mixture of designable structures with less designable ones. Hence, high σ is a better discriminator of high designability than high r . This difference between σ and r reflects the fact that distance from the mean σ better identifies the structures which are outliers from the distribution, and are hence likely to have high designability. We have thus found a quantity σ , determined purely from a single structure’s surface-exposure pattern, that can be used to identify highly designable structures.

The implication of having a quantity that can estimate designability from the properties of a single structure is that enumeration of a large set of competing structures is not necessary. This lifts the severe computational constraint that enumeration places on the size and complexity of structures that can be considered. In the remainder of this section, we study in more detail the relation between surface-exposure distance from the mean σ and the designability of structures. Our attention is focused on the possibility of identifying highly designable structures within a random sample, using either designability within the sample or distance from the mean σ .

Figure 7 shows the designability versus σ for chains of length $N = 15, 17$, and 19 . Over 10^6 sequences were generated to determine the designability of structures in each case. The

structures for each chain length were binned according to σ and the average designability of the structures in each bin is plotted. The correlation between σ and designability is clear, but there is an important caveat. We have only plotted the designability of structures which are the farthest from the mean in their own direction – this means that there are no other structures whose $\vec{\sigma}^\alpha$ has a greater projection onto the given structure’s direction $\vec{\sigma}$, *i.e.* $\vec{\sigma} \cdot \vec{\sigma}^\alpha < |\vec{\sigma}|^2$. for all other structures α . In this way, we have plotted only the “winners” in the winner-take-all competition for sequences that occurs when two or more structures have very similar patterns of surface exposure. In part, this procedure is justified to select only one member from every family of geometrically closely related structures.¹⁴ Fig. 8 illustrates the effect of this winner take all competition for the $N = 17$ case. Fig. 8(a) is a plot of designability versus σ for all structures, while Fig. 8(b) is a plot of designability versus σ for the “winning” structures, which are the farthest from the mean in their own direction. It can be seen that there are a large number of structures which have low designability despite having a large distance from the mean. Their designability has been reduced due to competition with a structure which is farther out on the hyper-plane. However, the structures with the largest values of distance from the mean σ are all highly designable.

In Fig. 7, the marked vertical lines on each graph indicate the values of σ for the 10th, 100th, and 1000th ranked structures according to σ in the *entire* set of compact structures. To highlight the significance of this in regards to random sampling, consider the following: if only 0.1% of the 17mer structures were sampled, it would still be expected that the 1000th ranked structure would occur in the sample. From the graph of the 17mer, even the 1000th ranked structure still has a reasonably high designability in that, on average, it is the ground state for a few hundred sequences. It is interesting to note that the designability versus σ curves become steeper as chain length N increases. Hence, it is reasonable to conclude that for larger protein structures, σ *improves* as a predictor of designability.

To emphasize how a structure’s location within fold space influences its designability, in Fig. 9 we present histograms of the number of nearby structures for the 1st, 100th, and least designable “winner” structures. To make these plots, we calculated the projections of all $\vec{\sigma}$ vectors onto the selected structure’s $\vec{\sigma}$ vector. The projections were normalized by the magnitude of the selected structure’s $\vec{\sigma}$. The histograms show the number of structures that have a given projection onto the chosen structure. Fig. 9(a) shows the histogram for the most designable 17mer structure. There is a large distance between it and the next nearest structure. However, for the less designable structures in Figs. 9(b) and (c) this distance is much shorter. In fact for the structure in Fig. 9(c), there are two other structures whose projections lie so close to the chosen structure as to fall into its own bin, of size 0.1. These near neighbors in fold space compete for sequences and are responsible for the low designability value.

Random sampling for 17mers – To show that highly designable structures can be identified within a sparse random sample we performed the following test. We randomly selected a set of 500 structures out of the complete set of 5000 compact 17mers. A designability calculation was then done for this small random sample. In Fig. 10(a), we plot the designability calculated using the complete set versus the designability in the random sample, for those structures that were the farthest out in their own direction. The correlation is good, with the highest designability structure correctly identified. The essential reason underlying the good agreement is the close correlation between designability and σ (cf. Fig. 7) combined

with the fact that σ for the random sample is effectively the same as σ for the complete set. This last relation is shown in Fig. 10(b), where we have re-evaluated the σ 's using the new mean $\langle \vec{r} \rangle$ of the random sample. The logic of random sampling is simple – we can identify highly designable structures from their large σ values, and only a small sample is required to calculate these σ 's. In fact, the designability for the complete set can be directly estimated from the σ values in the random sample, as shown in Fig. 10(c). The correlation is slightly better using the designability calculated within the random sample, as shown in Fig. 10(a), but the practical consideration of avoiding designability calculations may in some cases favor the direct use of σ values.

Random Sampling of Long-Chain Structures – We now show how to find candidates for highly designable long-chain structures by random sampling. For backbone configurations of length $N > 30$, complete enumeration of structures is infeasible. However, according to the results of the previous section, one can randomly sample long-chain structures, evaluate their surface exposures, and use the variation σ to estimate which ones are likely to be highly designable. Without the constraint of enumeration, one is free to consider more complex backbone configurations, for example, using a larger number of (ϕ, ψ) angle-pairs. In addition, the sampling of structures can be biased to favor configurations with realistic secondary structural elements.

To generate long-chain structures, we employed a set of four (ϕ, ψ) angle-pairs. The four pairs of angles were taken from high density regions of a Ramachandran plot: two pairs from the alpha-helical region, one from the beta-strand region, and the last from the left-handed alpha-helical region.³¹ Structures were generated by randomly selecting a pair of angles, weighted equally, and then randomly selecting proceeding angles from a transition table (Table 1), so that alpha-helical angles tend to follow alpha-helical angles, and beta-strand angles follow beta-strand angles. The matrix of transition probabilities in Table 1 was adapted from an analysis of transition probabilities between (ϕ, ψ) pairs of naturally occurring protein structures.³² The transition probabilities involving the left-handed alpha-helical angle were altered to include more turns to generate compact 30mers and 40mers for this study. As before, hard spheres were centered on each C_β position and self-avoidance was enforced by eliminating structures with overlapping spheres. We found that the use of the transition probabilities dramatically reduced the generation of self-intersecting structures.

We randomly sampled both 30mer and 40mer structures using the above procedure. For each length, the 500 most compact, self-avoiding structures generated in approximately two days of computing time on a 600 MHz PC were retained. Both the in-plane distance r and the distance from the mean σ were evaluated for the 500 structures in each random sample. Fig. 11 shows the top two 30mers and top two 40mers ranked by σ . According to the results of the previous section, these structures are our best candidates to be highly designable. We compare their values of σ to those of naturally occurring structures in the section below, and show that their structural characteristics are consistent with naturally occurring proteins.

An important caveat to the random sampling approach is that there could exist unsampled structures, with very similar patterns of surface exposure, that would compete for sequences with our top structures. Competing chain configurations that are *geometrically* similar can be considered as fluctuations of a single structure.¹⁴ However, the possibility of geometrically dissimilar structures with similar surface-exposure patterns, is an unavoidable uncertainty associated with random sampling. This competition for sequences between

geometrically dissimilar structures has been recently studied in lattice models.³³

Surface-Exposure Patterns of Naturally Occurring Structures – We now examine the surface-exposure patterns of naturally occurring proteins. From the Protein Data Bank (PDB), we selected groups of unrelated structures of fixed length N , with $N = 25 \dots 75$, and extracted their backbones. We then positioned uniformly sized spheres on the C_β positions, and evaluated surface exposure exactly as was done for the small chains studied above. Both the in-plane distance r and the distance from the mean σ were evaluated for the 71 natural occurring structures in the set.

Fig. 12(a) shows the length dependence of r for the selected set of natural protein structures using spheres with radius 1.9 Angstroms on the C_β positions. (We have chosen to plot r rather than σ since σ depends on the evaluation of $\langle \vec{r} \rangle$ which has a large error due to the small size of the sample). For small chains there is a broader variation than for the longer chains. This can be attributed to the fact that small proteins are often stabilized by disulfide bridges, rather than by the formation of a hydrophobic core.¹ In particular, for the $N = 25$ proteins, most structures had ill-defined cores, hence the lower values for the variance r . For larger proteins the distribution is narrower. This suggests that for larger proteins the hydrophobic force plays a more consistent role in creating a well-defined hydrophobic core. The average surface-exposure variation r decreases slightly with chain length. This could be anticipated from our normalization procedure: The total surface exposure for compact structures grows as $N^{2/3}$. If the variance of surface exposure of individual C_β spheres stays fixed, then the normalization implies $r_i^2 \sim N^{-4/3}$, and so $r \sim N^{-1/6}$ according to Eq. 4.

The highest r structures from the random sampling study above are shown as filled circles in Fig. 12(a). These structures lie at the high end of the variances of the naturally occurring proteins. This result is encouraging as it suggests that our best randomly generated structures share similar properties to real protein folds. However, the naturally occurring structures tend to be more open than the randomly generated structures. Hence, using small uniform spheres on the C_β positions overestimates the accessible regions of the natural structures. In Fig. 12(b), the in-plane distance of the selected 40mers from the PDB is shown as a function of side-chain sphere radius. Using larger spheres increases the variance and hence in-plane distance of the natural structures. Nevertheless, the top randomly sampled 40mer structure still falls within the mid to high range of the variance even when more realistic side-chain sphere sizes are used for the naturally occurring structures.

IV. CONCLUSIONS

In conclusion, we have shown that it is possible to estimate the relative designabilities of protein structures based on their exposed surface-area patterns, within an off-lattice model. Specifically, the *designability* of a structure – defined as the number of sequences with that structure as a unique lowest-energy state – was found to closely correlate with the surface-exposure variation of the structure. The ability to estimate designability from the properties of a single structure makes it unnecessary to completely enumerate structures. Instead, a sparse sample of structures can be generated, and relative designability assessed from designability within the sample, or directly from the surface-exposure variation of each structure. Random sampling, in turn, allows consideration of longer chains with greater

structural complexity. We have demonstrated the random sampling approach to designability for 30mers and 40mers. Our best candidates for highly designable structures were found to have surface-exposure variations similar to those of naturally occurring structures of the same size. Random sampling thus offers a promising way to find highly designable long-chain structures for ab initio protein design and also may be useful in the generation of decoys.

REFERENCES

- ¹ Creighton TE. Proteins. New York: Freeman, ed. 2; 1993. p. 236-237.
- ² Anfinsen CB. Principles that govern the folding of protein chains. *Science* 1973;181:223-230.
- ³ Chothia C. Proteins – 1000 families for the molecular biologist. *Nature* 1992;357:543-544.
- ⁴ Orengo CA, Jones DT, Thornton JM. Protein superfamilies and domain superfolds. *Nature* 1994;372:631-634.
- ⁵ Brenner SE, Chothia C, Hubbard TJP. Population statistics of protein structures: Lessons from structural classifications. *Curr. Opin. in Struct. Biol.* 1997;7:369-376.
- ⁶ Govindarajan S, Recabarren R, Goldstein RA. Estimating the total number of protein folds. *Proteins* 1999;35:408-414.
- ⁷ Finkelstein AV, Ptitsyn OB. Why do globular proteins fit the limited set of folding patterns? *Prog. Biophys. Mol. Biol.* 1987;50:171-190.
- ⁸ Yue K, Dill KA. Forces of tertiary structural organization in globular proteins. *Proc. Natl. Acad. Sci. USA* 1995;92:146-150.
- ⁹ Govindarajan S, Goldstein RA. Searching for foldable protein structures using optimized energy functions. *Biopolymers* 1995;36:43-51.
- ¹⁰ Li H, Helling R, Tang C, Wingreen N. Emergence of preferred structures in a simple-model of protein-folding. *Science* 1996;273:666-669.
- ¹¹ Li H, Tang C, Wingreen NS. Are Protein Folds Atypical? *Proc. Natl. Acad. Sci. USA* 1998;95:4987-4990.
- ¹² Mélin R, Li H, Wingreen NS, Tang, C. Designability, thermodynamic stability, and dynamics in protein folding: a lattice model study. *J. Chem. Phys.* 1999;110:1252-1262.
- ¹³ Bornberg-Bauer E, Chan HS. Modeling evolutionary landscapes: Mutational stability, topology, and superfunnels in sequence space. *Proc. Natl. Acad. Sci.* 1999;96:10689-10694.
- ¹⁴ Miller J, Zeng C, Wingreen NS, Tang C. Emergence of highly-designable protein-backbone conformations in an off-lattice model. Available in public e-print archive accessible at <http://xxx.lanl.gov> and referenced by cond-mat/0109305 (2001).
- ¹⁵ Lau KF, Dill KA. A lattice statistical mechanics model of the conformational and sequence spaces of proteins. *Macromolecules* 1989;22:3986-3997.
- ¹⁶ Chan HS, Dill KA. The effects of internal constraints on the configurations of chain molecules. *J. Chem. Phys.* 1990;92:3118-3135.
- ¹⁷ Shakhnovich E, Gutin A. Enumeration of all compact conformations of copolymers with random sequence of links. *J. Chem. Phys.* 1990;93:5967-5971.
- ¹⁸ Camacho CJ, Thirumalai D. Minimum energy compact structures of random sequences of heteropolymers. *Phys. Rev. Lett.* 1993;71:2505-2508.
- ¹⁹ Pande VS, Joerg C, Yu Grosberg A, Tanaka T. Enumerations of the Hamiltonian walks on a cubic sublattice. *J. Phys. A* 1994;27:6231-6236.
- ²⁰ Park BH, Levitt M. The complexity and accuracy of discrete state models of protein structure. *J. Mol. Biol.* 1995;249:493-507.
- ²¹ Kauzmann W. Some factors in the interpretation of protein denaturation. *Adv. Protein Chem.* 1959;14:1-63.
- ²² Dill KA. Dominant forces in protein folding. *Biochemistry* 1990;29:7133-7155.

- ²³ Li H, Tang C, and Wingreen NS. Nature of driving force for protein folding: a result from analyzing the statistical potential. *Phys. Rev. Lett.* 1997;79:765-768.
- ²⁴ Nozaki Y, Tanford C. The solubility of amino acids, diglycine, and triglycine in aqueous guanidine hydrochloride solutions. *J. Biol. Chem.* 1971;246:2211-2217
- ²⁵ Levitt M. Simplified representation of protein conformations for rapid simulation of protein folding. *J. Mol. Biol.* 1976;104:59-107
- ²⁶ Roseman MA. Hydrophilicity of polar amino acid side-chains is markedly reduced by flanking peptide bonds. *J. Mol. Biol.* 1988;200:513-522.
- ²⁷ We evaluate the area of each C_β sphere accessible to a water ball of radius 1.4 Angstrom, *cf.* Flower DR. *J. Mol. Graph. Model.* 1997;15:238.
- ²⁸ The discarded structures are too open to have well defined cores and therefore have low designabilities, as discussed in Section III.
- ²⁹ Eisenberg D, McLachlan AD. Solvation energy in protein folding and binding. *Nature* 1986;319:199-203.
- ³⁰ Buchler NEG, Goldstein RA. Surveying determinants of protein structure designability across different energy models and amino-acid alphabets: A consensus. *J. Chem. Phys.* 2000;112:2533-2547.
- ³¹ The four (ϕ, ψ) angles chosen were: $\alpha_1 = (-45, -55)$, $\alpha_2 = (-70, -20)$, $\beta = (-100, 100)$, and $L = (50, 25)$ based on a clustering method given in Ref.³².
- ³² J. Miller, private communication.
- ³³ Kaya H, Chan HS. Polymer principles of protein calorimetric two-state cooperativity. *Proteins* 2000;40:637-661.

TABLES

Transition Probabilities between Dihedral Angle-Pairs

$angle_1 \backslash angle_2$	α_1	α_2	β	L
α_1	0.65	0.30	0.0	0.05
α_2	0.35	0.35	0.2	0.10
β	0.1	0.1	0.8	0.0
L	0.09	0.1	0.8	0.01

TABLE I. Transition probabilities Probability(column|row) for successive angle-pairs for the four (ϕ, ψ) pairs used³¹ to generate 30mer and 40mer structures

FIGURES

FIG. 1. Depiction of a 19mer structure, constructed using the three (ϕ, ψ) angle-pairs described in the text. The amino-acid side groups are modeled by self-avoiding spheres of radius 1.9\AA centered on the C_β positions.

FIG. 2. Schematic diagram of fold space. Black circles correspond to vectors of exposed surface area \vec{a} for individual structures. Since the surface-area vectors are normalized, all lie on a single hyper-plane. The vector for uniform exposed area $\vec{n} = (1/N, \dots, 1/N)$ is the origin for all vectors on the hyper-plane. The in-plane vector $\vec{r} = \vec{a} - \vec{n}$ is shown for one structure (labelled “S”) with a large $|\vec{r}|$, and thus a highly non-uniform exposed surface area. For the same structure, the vector $\vec{\sigma} = \vec{r} - \langle \vec{r} \rangle$, relative to the mean of the distribution $\langle \vec{r} \rangle$, is also shown. Structures with surface-exposure patterns very different from the mean, and thus with large values of $|\vec{\sigma}|$, are typically highly designable. The sequences which have “S” as their lowest-energy conformation, and thus contribute to the designability of “S”, are shown schematically by the shaded “hyper-cone”.

FIG. 3. Histogram of designability for the 5000 most compact, self-avoiding 17mers. The histogram has an exponentially decreasing tail of highly designable structures.

FIG. 4. Normalized exposed surface area versus position of monomer on chain, averaged over the 5000 most compact, self-avoiding 17mer structures. The dashed straight line corresponds to the uniformly exposed structure $(1/17, 1/17, \dots, 1/17)$. Also shown is a typical normalized surface exposure pattern of a compact structure (dot-dash)

FIG. 5. Histogram of surface-exposure-variation magnitude r for all self-avoiding 17mers (solid line) and for the 5000 most compact, self-avoiding 17mers (dotted line).

FIG. 6. Plot of distance from the mean σ against in-plane distance r for the 5000 most compact, self-avoiding 17mers. Black circles correspond to the 50 topmost designable structures and white squares to structures that are less designable.

FIG. 7. Plot of designability versus distance from the mean σ for “winner” structures of length $N = 15, 17,$ and 19 . Error bars indicate the uncertainty in designability for each bin. The vertical lines correspond to the 10th, 100th, and 1000th structures ranked according to σ in the entire sample.

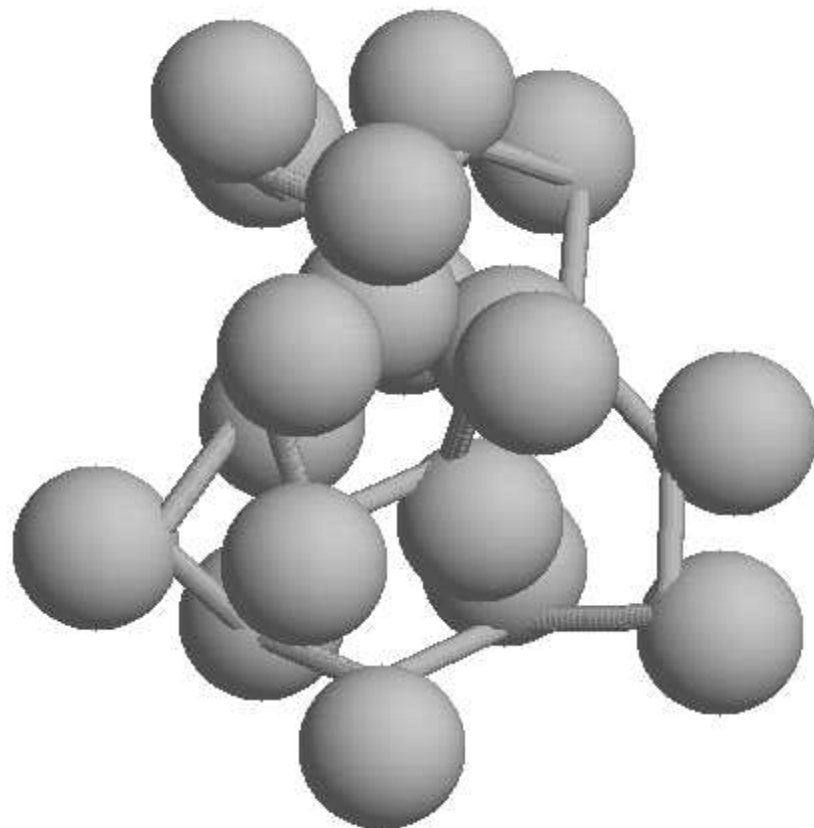
FIG. 8. (a) Plot of designability versus distance from the mean σ for all structures of length $N = 17$. (b) Plot of designability versus distance from the mean σ for “winner” structures of length $N = 17$, *i.e.* those structures which lie the farthest out in their own direction.

FIG. 9. Histograms of the normalized projections of the $\vec{\sigma}$'s of all 17mer structures onto the $\vec{\sigma}$ of the (a) most designable, (b) 100th most designable, and (c) least designable “winner” structure. Note the change of y -axis scale in (c).

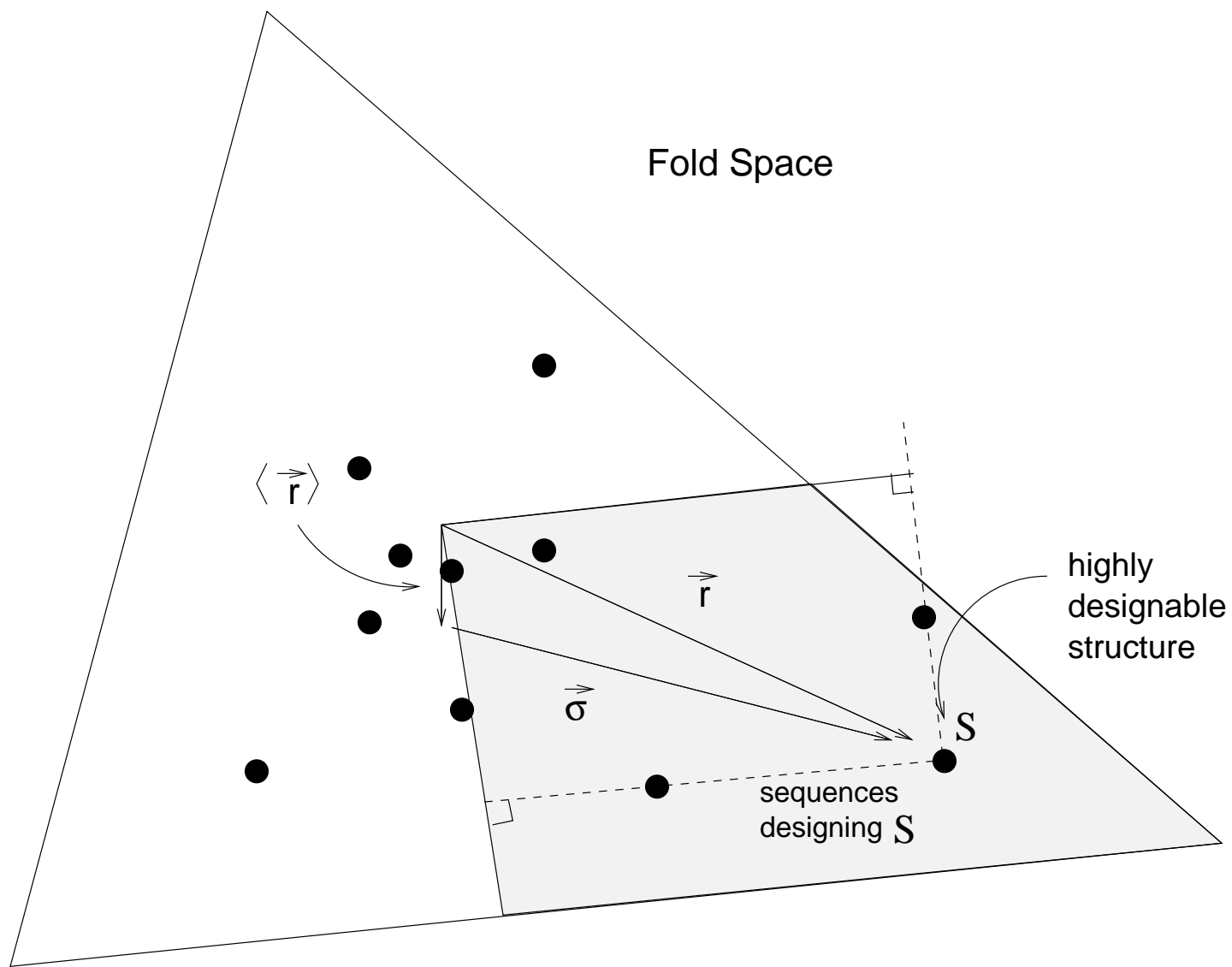
FIG. 10. (a) Plot of designability in the full set of 5000 compact, self-avoiding 17mers versus designability calculated for a random sample of 500 of these structures. Of the sampled structures, only those that are the farthest out in their own direction on the hyper-plane are shown. (b) Plot of surface-exposure distance from the mean σ in the full set versus σ for the same random sample of 500 structures. (c) Plot of designability in the full set versus σ in the random sample.

FIG. 11. Top structures ranked according to surface-exposure distance from the mean σ in sparse random samples of 30mers and 40mers: (a),(b) top two ranked 30mers according to σ ; (c),(d) top two ranked 40mers according to σ .

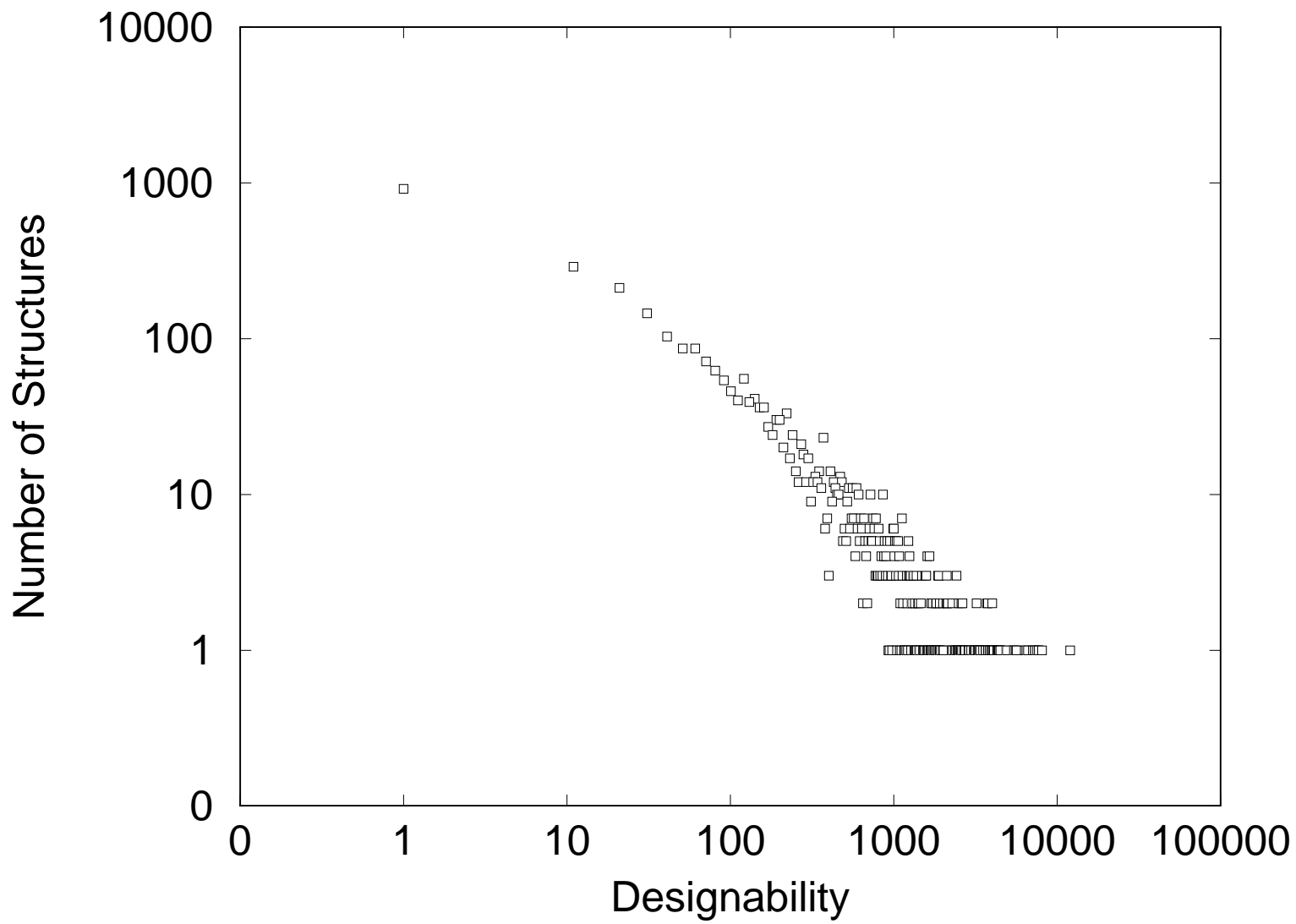
FIG. 12. (a) Surface-exposure distance from the in-plane distance r for naturally occurring protein backbones in the Protein Data Bank for $N = 25 - 75$. For each N , only structurally distinct proteins in the Data Bank were selected. Also shown in black circles are the values of r for the top 30mer and 40mer from the randomly generated structures shown in Fig. 11. (b) The dependence of r on choice of side-chain sphere radius for the set of selected 40mers in the PDB. The value of r of the top randomly generated 40mer is shown as a black circle.



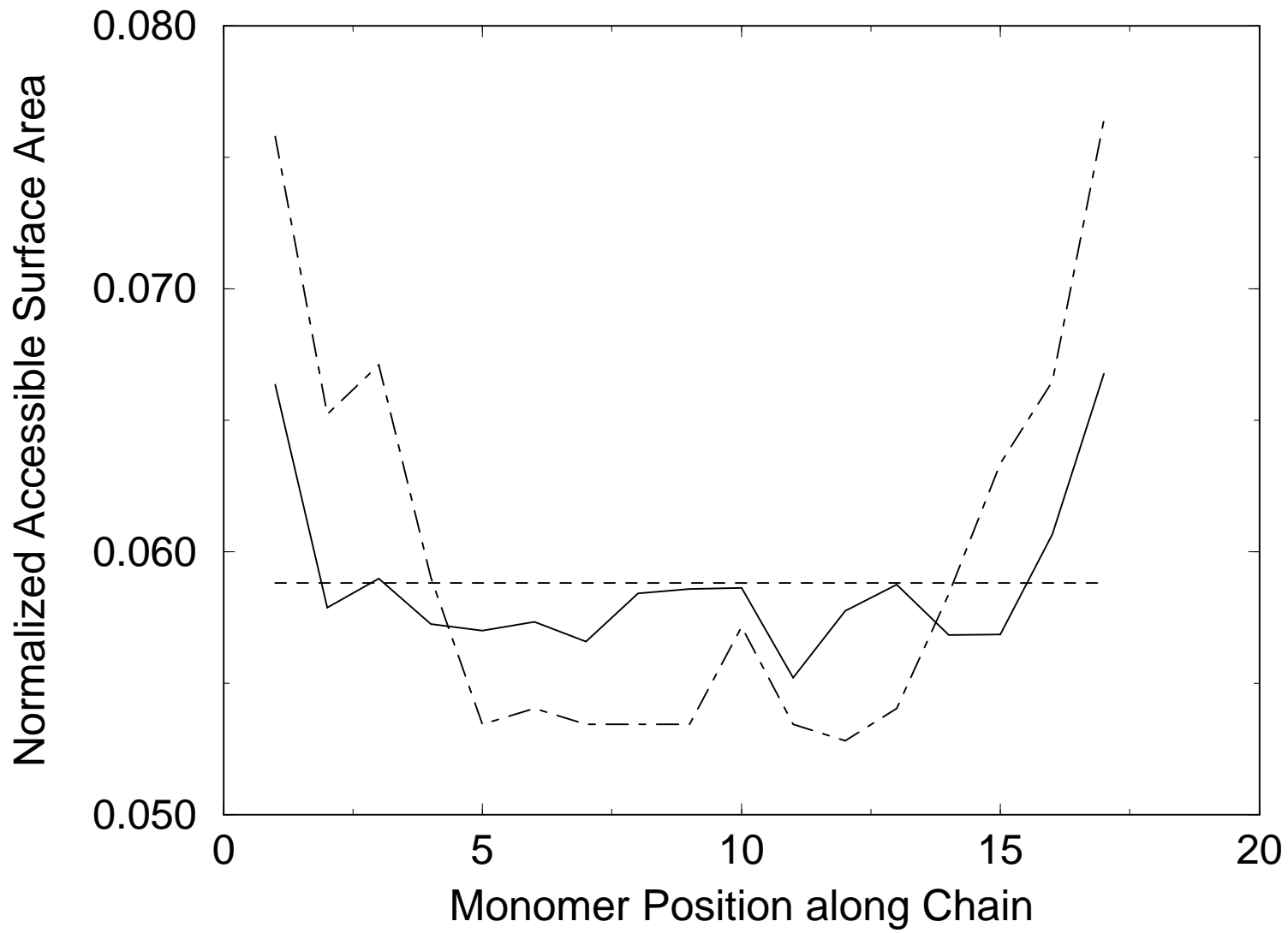
Emberly et al Fig. 1



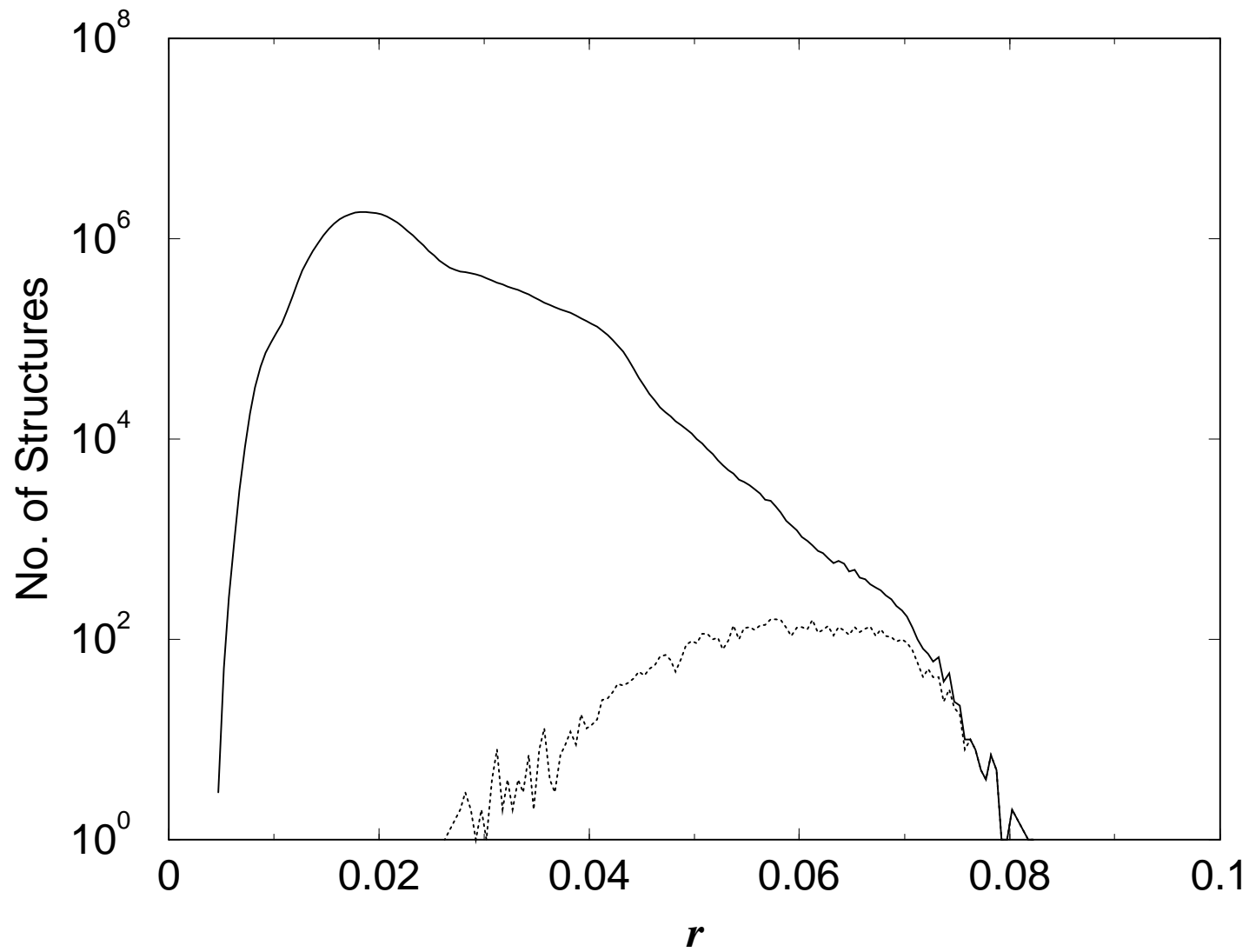
Emberly et al. Fig. 2



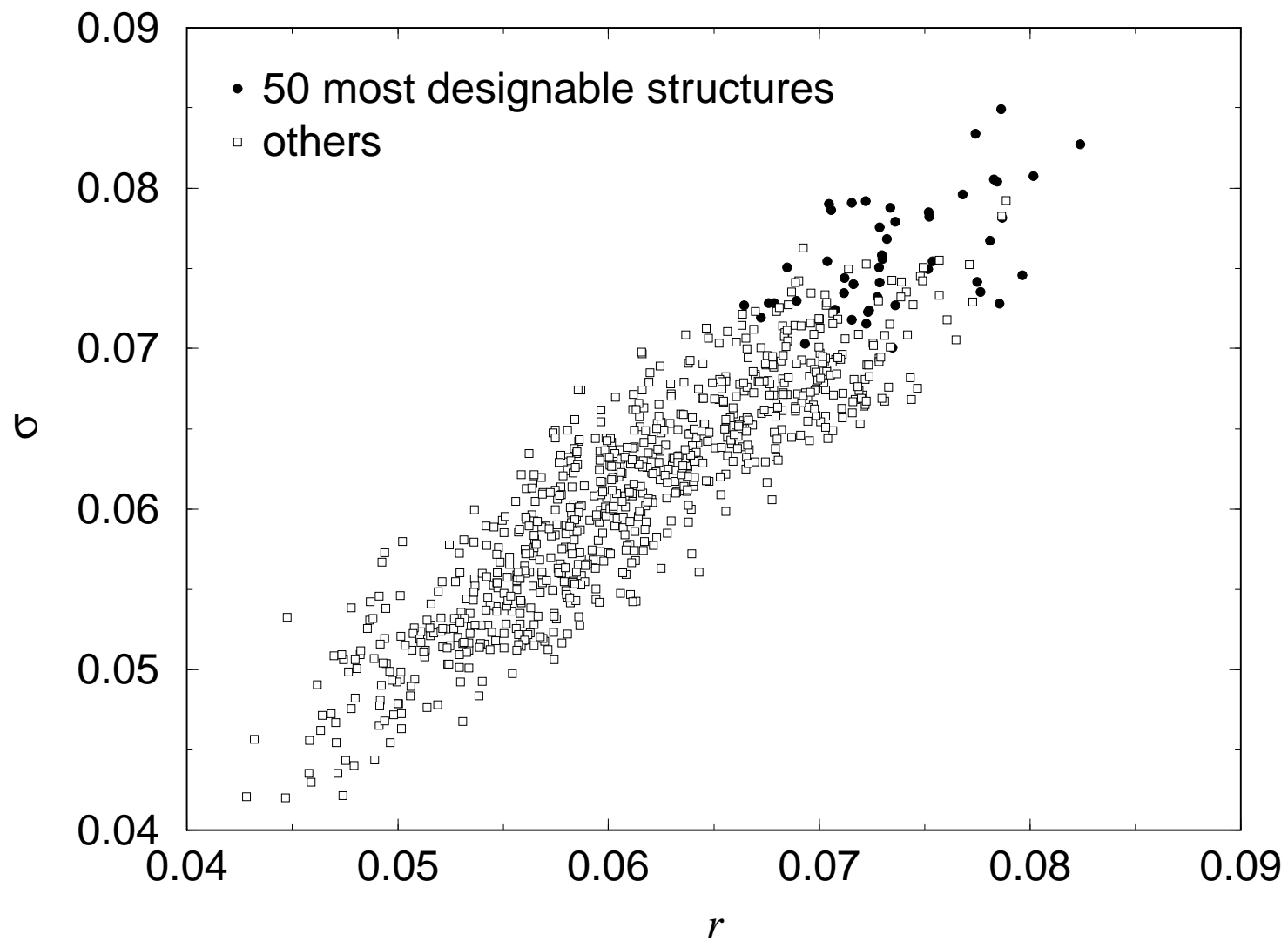
Emberly et al. Fig. 3



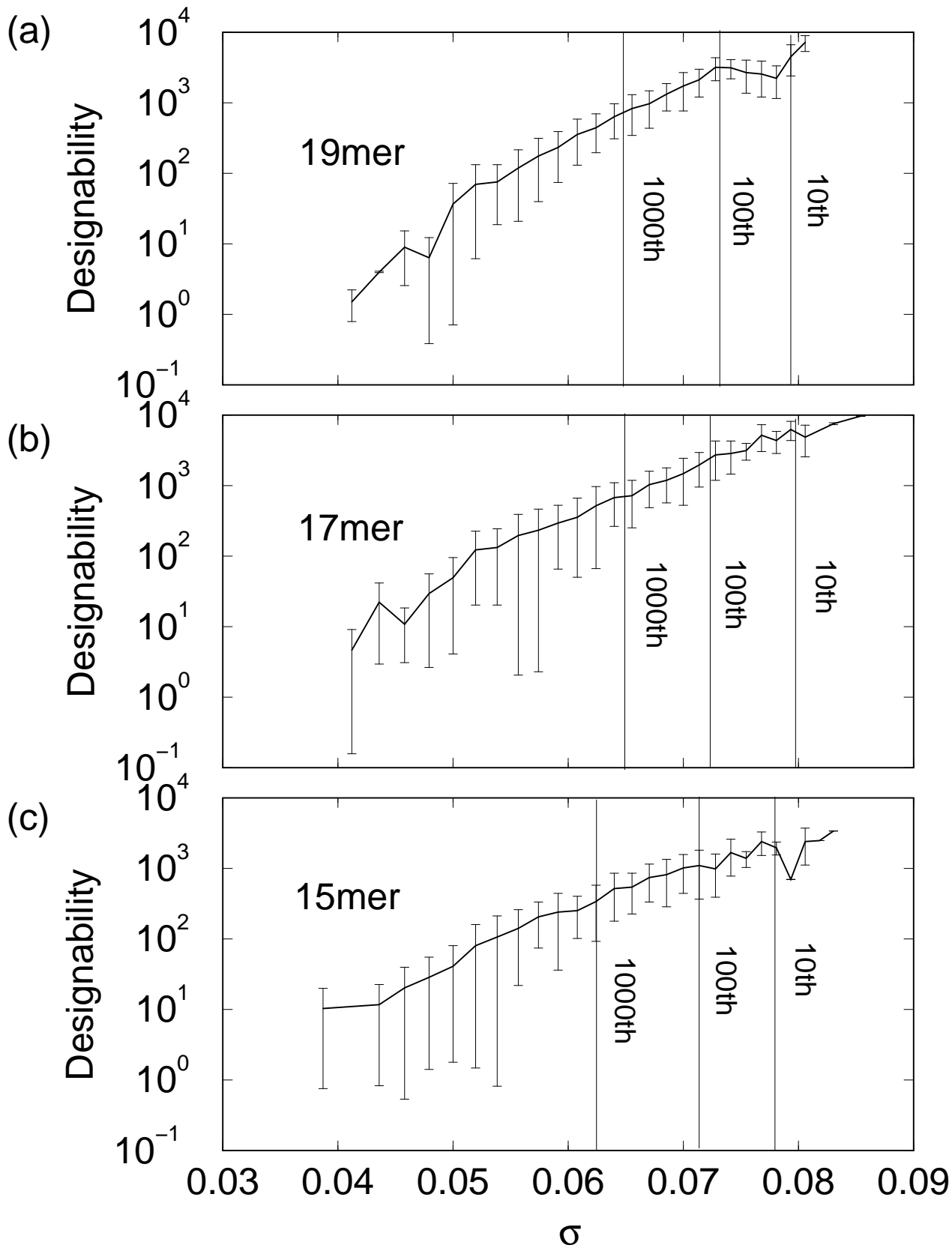
Emberly et al. Fig. 4



Emberly et al. Fig 5

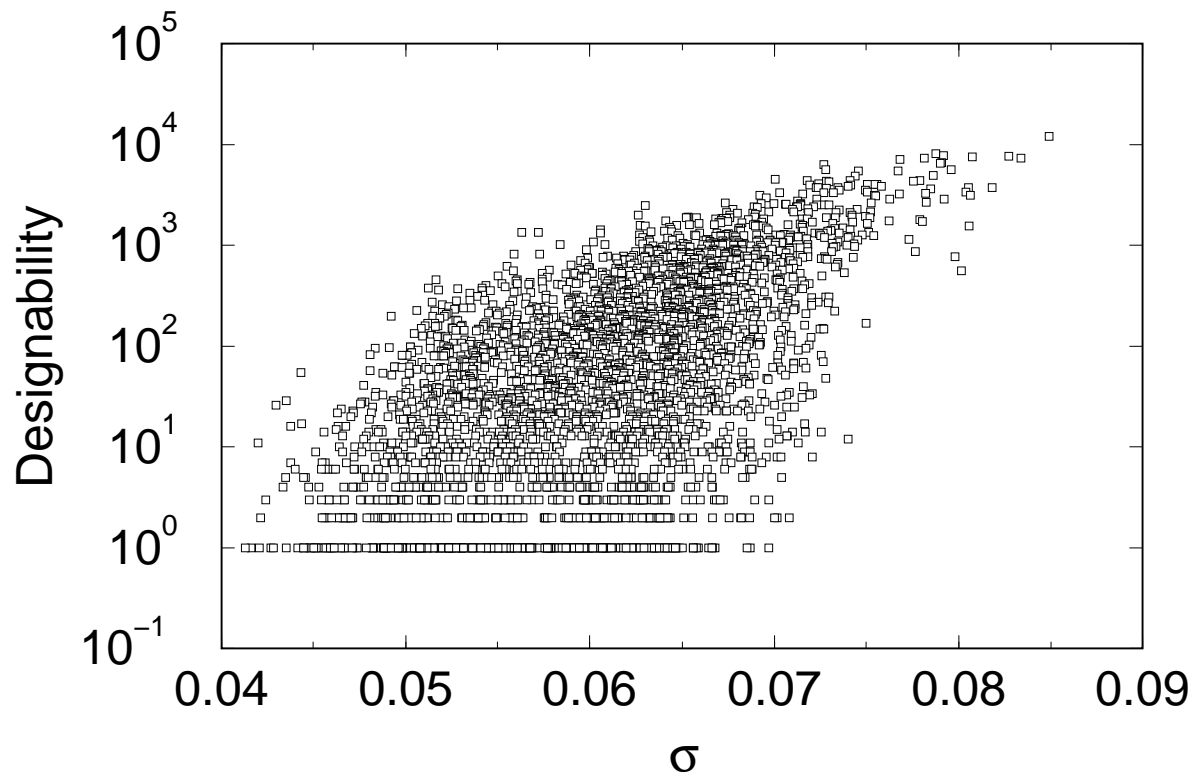


Emberly et al Fig. 6

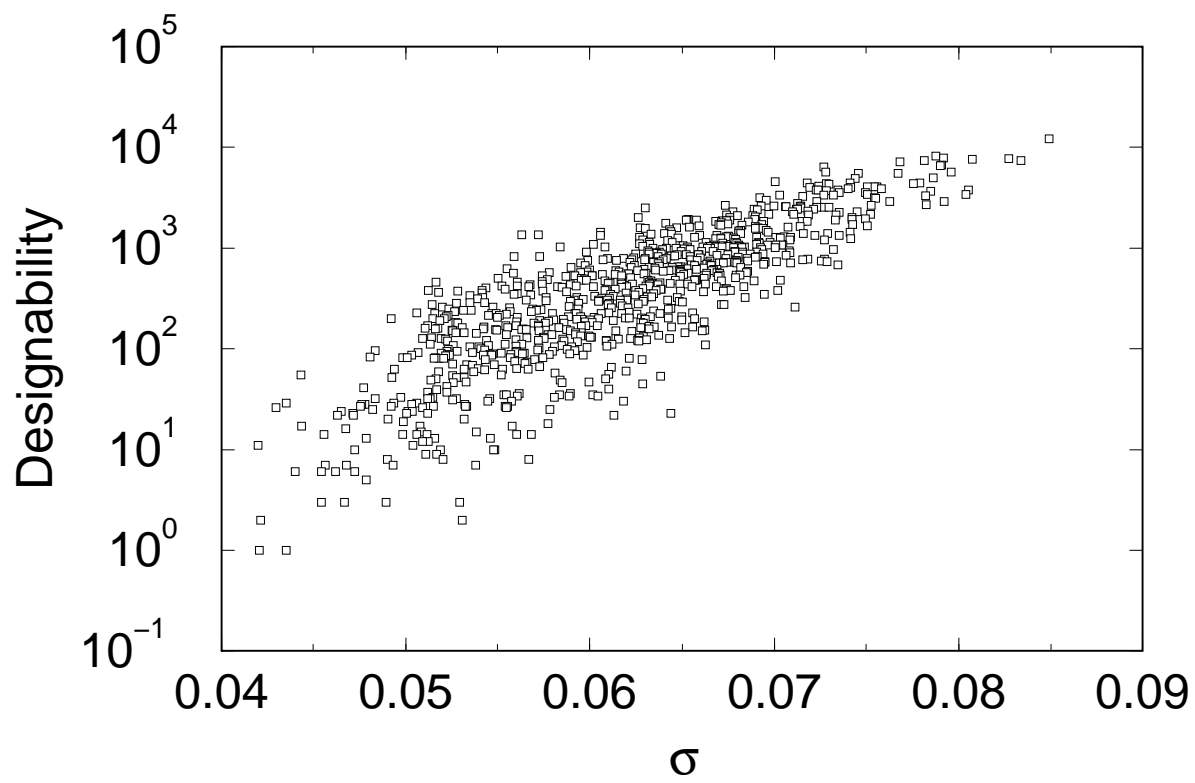


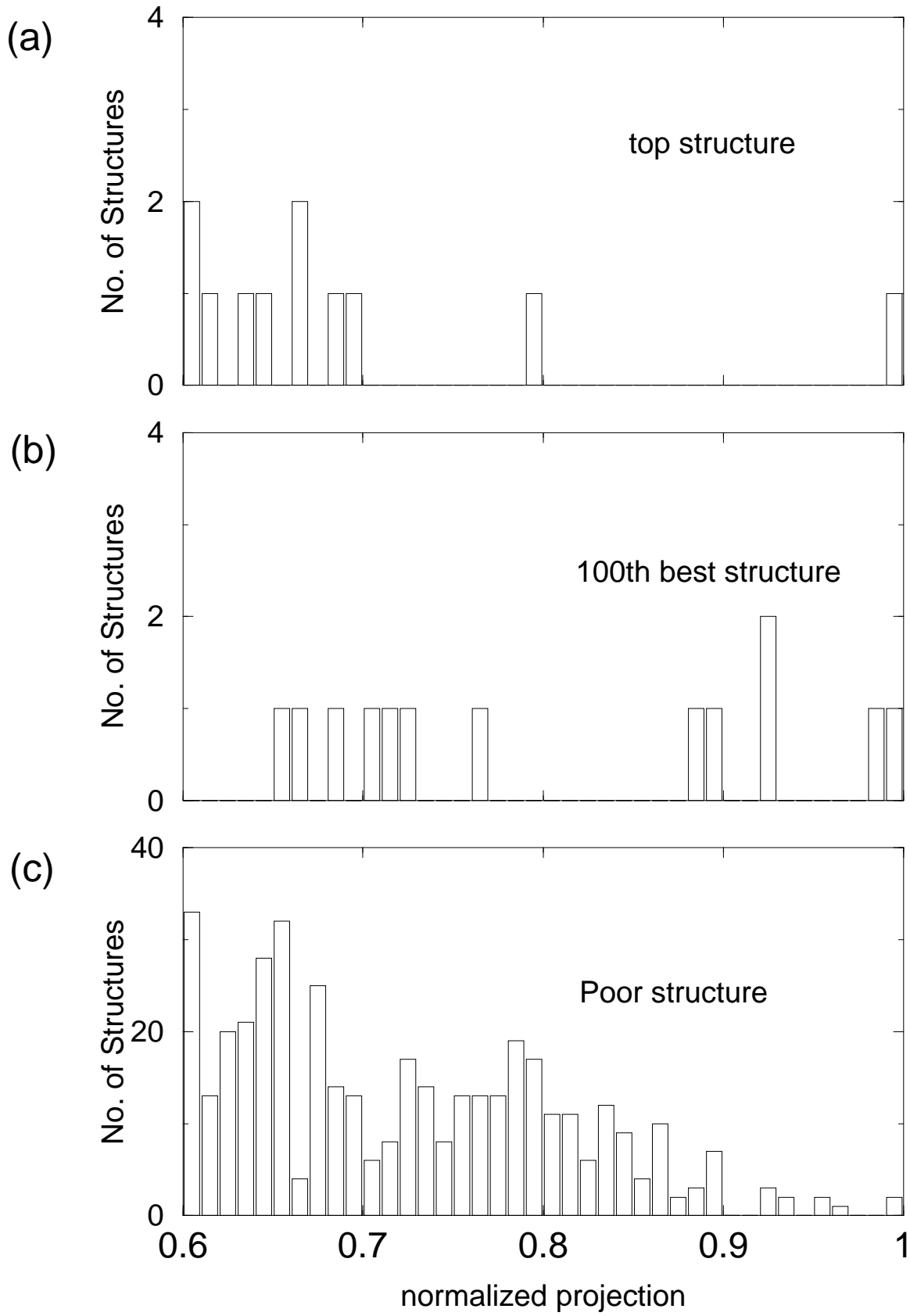
Emberly et al Fig. 7

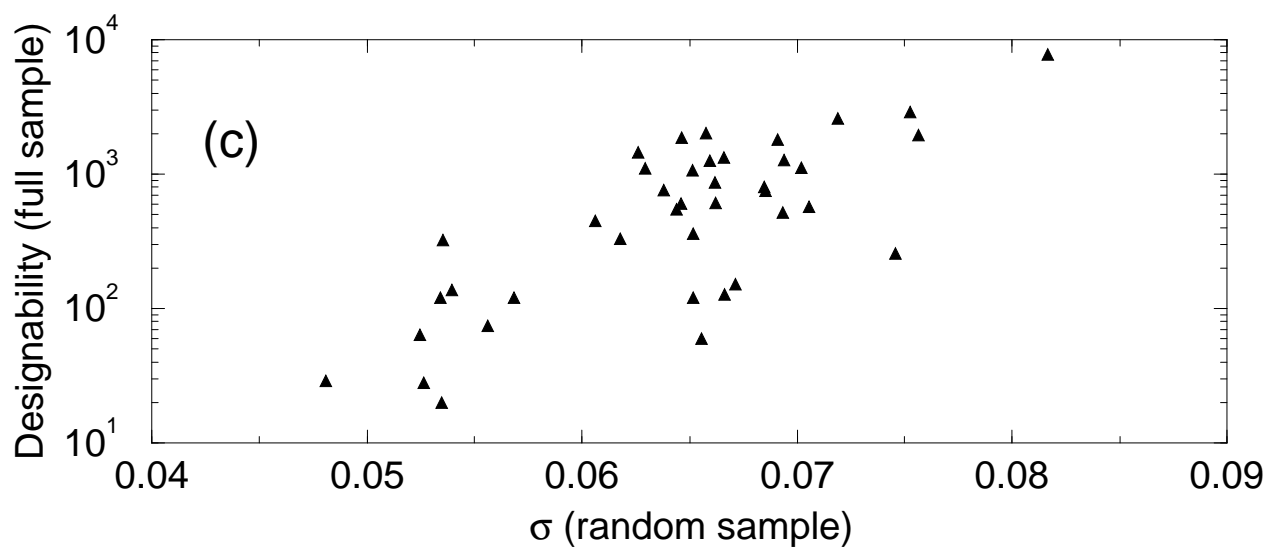
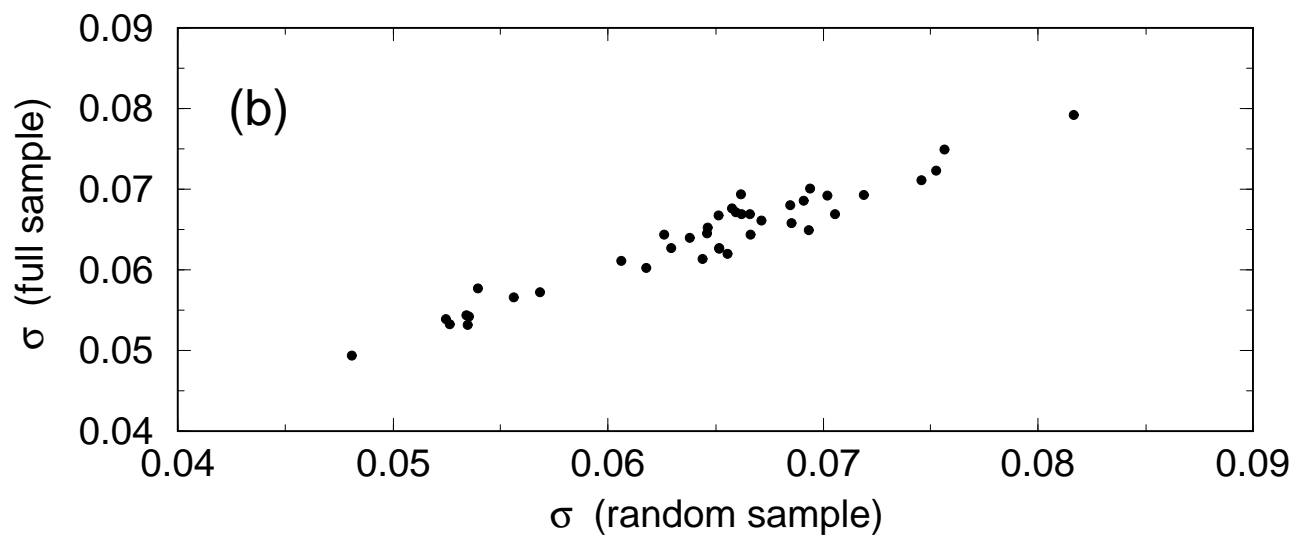
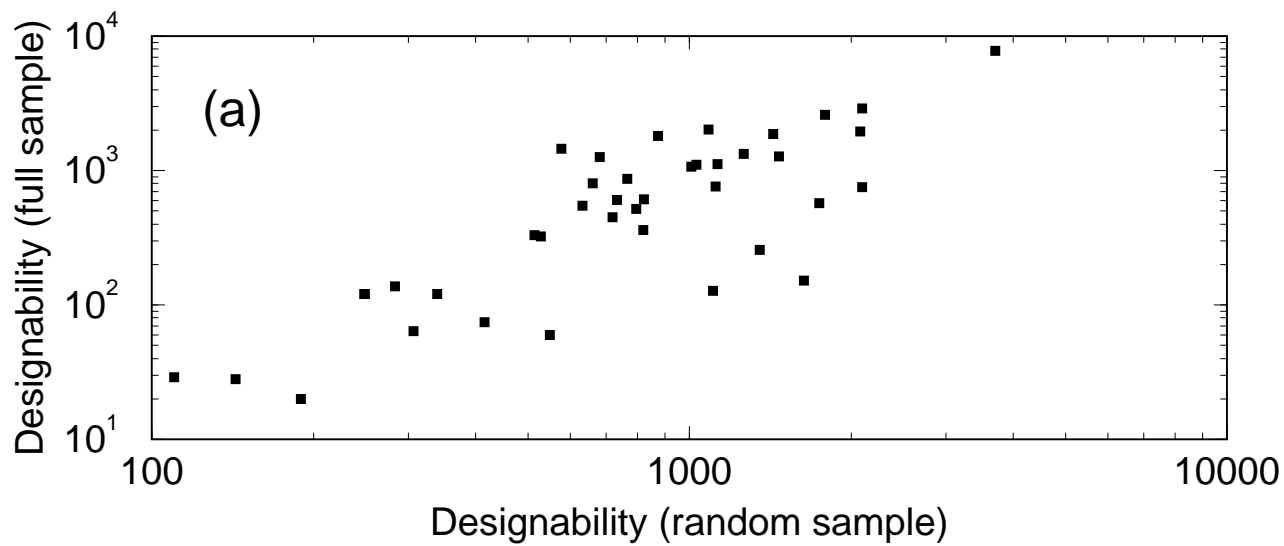
(a)



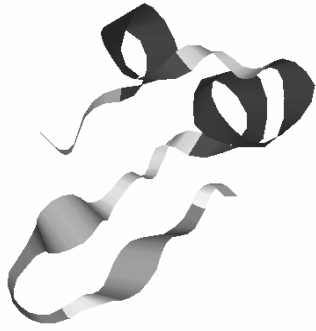
(b)







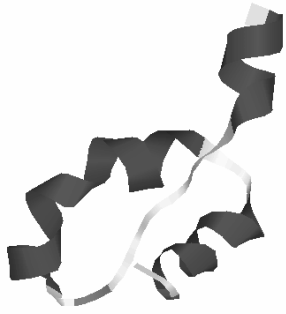
a)



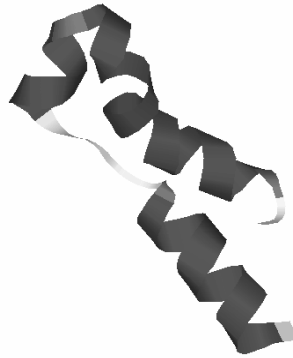
b)



c)



d)



Emberly et. al. Fig. 11

